Powder Technology 286 (2015) 84-89

The development of powder injection moulding binders: A quantification of individual components' interactions

D. Bleyan[a,b], B. Hausnerova[a,b,*], P. Svoboda[b,c]

[a] *Department of Production Engineering, Faculty of Technology, Tomas Bata University in Zlin, nam. T.G. Masaryka 5555, 760 01 Zlin, Czech Republic*
[b] *Centre of Polymer Systems, University Institute, Tomas Bata University in Zlin, Nad Ovcirnou 3685, 760 01 Zlin, Czech Republic*
[c] *Department of Polymer Engineering, Faculty of Technology, Tomas Bata University in Zlin, nam. T.G. Masaryka 275, 762 72 Zlin, Czech Republic*

Abstract

The study of interactions between binder system components is critical for improving the processing properties of powder injection moulding (PIM) feedstocks. In this paper the interactions between acrawax (AW) and polyethylene glycol (PEG) were analysed and compared with those obtained for carnauba wax (CW). Due to the complexity of interaction mechanisms, the polymers were substituted with their basic low molecular weight analogues and analysed by FTIR and calorimetry. Self-interaction energies and association energies were determined using calorimetric analysis. Shifts of FTIR absorption peaks (C-O stretch and N-H stretch) served as evidence of the presence of interactions between the components. The calorimetric study of AW/PEG analogues showed a temperature increase during mixing, indicating the presence of strong interactions. The combined data from FTIR and calorimetry allowed a quantitative evaluation, which indicated about two times stronger interactions between AW (with C=O and N–H groups) and PEG (with C–O and –OH groups), as compared to CW (with C=O and C–O groups) and PEG analogues.

Keywords

Powder injection moulding, Binder, Low molecular weight analogue, Specific interactions, FTIR, Calorimetry

* Corresponding author at: Department of Production Engineering, Faculty of Technology, Tomas Bata University in Zlin, nam. T.G. Masaryka 5555, 760 01 Zlin, Czech Republic.
E-mail address: hausnerova@ft.utb.cz (B. Hausnerova).

http://dx.doi.org/10.1016/j.powtec.2015.07.046

1. Introduction

In recent years, powder injection moulding (PIM) has established itself as a cost-effective production technique derived from plastic injection moulding, allowing large scale production of complex parts. The binder system in PIM plays an important role, bestowing on the feedstock the required processing properties and ensuring defect-free processing throughout each production stage [1].

Suitable processing properties of a powder feedstock are usually achieved by using a binder system consisting of up to 5 different polymers and waxes, which complicates the investigation of the complete and individual reaction pathways and the chemical mechanisms occurring within such a system. The majority of binder systems is based on polyolefin backbones such as polyethylene (PE) or polypropylene (PP), and includes also polyethylene glycols (PEGs) with various molecular weights and waxes such as paraffin wax (PW).

Despite the substantial effort made in studying PE and PP binders [e.g. 2], their usage often leads to processing issues such as insufficient initial pore formation and weak internal transport mechanisms within the green parts, resulting in lower debinding rates. PEG's main role is as plasticiser [3]; besides improving the viscoelastic properties its use is endorsed by water solubility allowing an environmentally safe debinding process [4] (in contrast to PW, which dissolves in heptane, hexane, or kerosene [5]).

At present, the binder's properties are assessed by rheological measurements and thermogravimetry [6-11]. There is a noticeable lack of research effort in the area of specific interactions among the particular binder system components. In order to improve the feedstock properties, mathematical models for predicting the feedstock properties or substituting conventional processing stages by implementing sophisticated techniques requiring the merging of two consequent stages are employed. However, even the latter approach can be justified if an outsourced and intensive study of the adhesion of binder to powder, and the interactions between binder components are performed prior to it.

Various techniques were exploited for studying the interactions in polymer blends. Chen and Wolcott [12] reported on a study of interaction parameters for polymer-diluent systems of PW and PE (HDPE, LDPE and LLDPE). The morphology, crystallization and crystallinity together with equilibrium melting temperature and melting point depression were analysed using differential scanning calorimetry and atomic force microscopy. The results showed evidence of partial miscibility of blends, with LLDPE having an advantage over HDPE and LDPE.

Doulabi et al. [13] studied the miscibility of PEG and chitosan by using an acetate buffer solution for different blend compositions. Viscosity, density, and refractive index were measured in order to quantify the interaction parameters. The results showed that the components at 80% or higher chitosan concentration were miscible by means of the intermolecular hydrogen-bonding interaction between hydroxyl groups of polyethylene glycol fumarate with amino and hydroxyl groups of chitosan.

In our previous research, polar waxes were exploited as binder system components applicable to the PIM process [14] to substitute nonpolar PE and PW with the aim of eliminating the necessity to use processing aid, e.g., stearic acid (SA), in order to achieve the adhesion of the binder to the powder required to withstand high shear forces during injection moulding. Similarly to the most recent work by Liu et al. [15], who substituted paraffin wax with bee wax for the production of micro-injection moulding gears from zirconia, better feedstock stability has been achieved. However, with such novel binders, an understanding of core mechanisms of interactions between the individual system components would allow a precisely-balanced composition, bringing the feedstock properties to their higher limits (e.g., substantially lowering the processing temperatures in the case of substitution of PE by carnauba wax (CW) or acrawax(AW)) [14].

While quantification of the interactions of two polymers is a difficult task, in the case where both polymers are polar it becomes even more challenging. This is because the interactions between polymer (*X*) and polymer (*Y*) are significantly weaker than the self-interactions *X*–*X* and *Y*–*Y* in each polymer. To bypass this issue, polymers might be substituted with low molecular weight analogues to have an advantage of eliminating the majority of self-interactions, and replacing them with newly formed *X*–*Y* interactions. This rarely used [16,17] approach allows the substitute liquid for the *X* polymer to be fully surrounded by the substitute liquid for the *Y* polymer, resulting in precise measurements of the present interactions. Furthermore, the calorimetric analysis combined together with Fourier transform infrared spectroscopy (FTIR) measurements can provide a quantitative evaluation of specific interactions.

Some researchers have reported on the successful use of FTIR or calorimetry techniques for quantifying and evaluating interactions [18-20]. To our best knowledge, no research has yet been performed on the miscibility of PEG and polar waxes.

In our previous paper [21], we tested this approach to verify the presence of interactions between CW and PEG low molecular substitutes. Motivated by the work of Hsu et al. [22] who compared CW and AW in 56 vol.% 304L stainless steel feedstocks containing 22 vol.% of low density polyethylene (LDPE), and from the separation and aggregation of LDPE molecules from the binder during mixing, it was speculated that AW, containing strong polar amide groups and short hydrocarbon chain ends, was less compatible with LDPE than CW. The aim to quantify the interaction potential of both waxes increased.

Thus, in this work, the interactions between AW and PEG are examined and compared to those employed in our novel powder feedstock [14] based on CW/PEG in order to investigate whether the approach of low molecular weight analogues treated with combined FTIR/calorimetry is able to intercept the slight differences in behaviour viewed by other techniques currently used (rheometry and thermogravimetry).

2. Experimental

2.1 Materials

Table 1 shows the low molecular weight analogues of AW, CW and PEG used in this study. The molar mass M_w, density ρ, and the specific heat capacity c_p of analogues are shown in Table 2. As buffer solutions (solvents), hexane and decahydronaphthalene (decalin) were used. The chemicals were obtained from Sigma-Aldrich.

2.2 Methodology

The quantitative analysis of interactions is based on the assumption that the change of Van der Waals intermolecular interactions accompanying mixing is negligible (e.g., the mixing of hexane and heptane) and all contributions to the heat of mixing are due to specific acid-base interactions, as well as that all organic liquids (except for saturated hydrocarbons) make the specific self-association based on electron donor (basic) and electron acceptor (acid) sites of one molecule, all *X*–*X* interactions are broken in the case of high dilution, all dissociated *X* molecules form new *X*–*Y* interactions, and finally, molecules *Z* (saturated hydrocarbons) do not have any acid-base self-associations, nor do they form acid-base interactions with another molecule (*X* or *Y*) [23].

Table 1
Low molecular analogues of corresponding polymers.

Name	Abbreviation	Chemical structure
Acrawax	AW	$CH_3(CH_2)_{16}CNHCH_2CH_2NHC(CH_2)_{16}CH_3$ (O, O)
Analogue Methylacetamide	NMA	CH_3CNHCH_3 (O)
Carnauba wax	CW	$H_3C–(CH_2)_{30}–C–O–(CH_2)_{33}CH_3$ (O)
Analogues Amyl butyrate	AM	$CH_3\text{-}CH_2\text{-}CH_2\text{-}C\text{-}O\text{-}CH_2\text{-}CH_2\text{-}CH_2\text{-}CH_2\text{-}CH_3$ (O)
Butyl valerate	BV	$CH_3\text{-}CH_2\text{-}CH_2CH_2\text{-}C\text{-}O\text{-}CH_2\text{-}CH_2\text{-}CH_2\text{-}CH_3$ (O)
Polyethylene glycol	PEG	$H–\left[–CH_2\text{-}CH_2–\right]_n H$
Analogues 2-Ethoxyethanol Diethylene glycol monoethyl ether	2ET DGME	$C_2H_5OCH_2CH_2OH$ $C_2H_5OCH_2CH_2OCH_2CH_2OH$

2.2.1. FTIR analysis

The *X–X* self-interactions and *X–Y* interactions between two liquids were studied using FTIR analysis. An FTIR reflection spectroscope (Nicolet 6700, Fisher Scientific, USA) equipped with a KBr glass holder accessory was used. A drop of each mixture was placed between two KBr glasses and measured in a transmission mode. The spectra with 32 scans were collected in the range of 400-4000 cm^{-1} at the resolution of 1 cm^{-1}. The procedure was repeated three times, and the results were averaged.

2.2.2. Calorimetry

A thermocouple (type copper-constantan) was connected to National Instruments data acquisition equipment (NIUSB-9211A, Data Acquisition for Thermocouples) and used for measuring the temperature change during the mixing. LabVIEW Signal Express 2.5 software was used for collecting the temperature with a precision of 0.0001 °C. A 0.5 s sampling period was applied. The thermocouple was dipped in the blend, which was placed on a hot plate in the insulated flask with a magnetic stir rotating at 250 rpm. To achieve a 1% concentration of the blend, 0.05 ml of liquid *X* was diluted in 5 ml of liquid *Y*. The temperature change during mixing was measured, and the time-temperature curve was evaluated.

Table 2
Physical properties of low molecular liquid substitutes

Name	Molar mass M_w [g/mol]	Density ρ [g/cm^3]	Heat capacity $C\rho$ [J/kg K]
AW	593.02	0.97	2910
Analogue			
NMA	73.09	0.957	3748
CW	1000	0.97	3373
Analogues			
AM	158.24	0.863	1927
BV	158.24	0.868	1927
PEG	1000-20,000	1.09 - 1.41	2200-2460
Analogues			
2ET	90.12	0.930	2414
DGME	134.17	0.999	2193

3. Results and discussion

Low molecular weight liquids were diluted at various concentrations in order to define the optimal dilution ratio. The results demonstrated that a 1% dilution was optimal for both *X–X* and *X–Y* combinations. The shift of the N–H stretch peak was considered for AM-NMA and BV-NMA substitute liquid blends. Previously collected data [21] for CW and PEG substitute peak shifts of –OH and C=O stretch peaks were used for comparison. The obtained data showed that the NMA peak shift for the N-H amino group in the range of 3050 to 3440 cm^{-1} was higher in decalin (see Table 3), similar to CW low molecular analogues, while being significantly smaller in hexane, vice versa to the peak shift of PEG analogues. It is also noticeable that the peak shift was more significant for the second minor peak (Fig. 1). Both major and minor N–H peaks of NMA in hexane and decalin tended to a lower wavenumber, which is often referred to as proof of the presence of interactions [24]. However, when blended with AM and BV, the major peak tended to a higher wavenumber, which can be explained as repulsive interactions between components. The C–O stretch absorption peak at 1125 cm^{-1} for NMA expressed a similar trend to shift to lower wavenumbers for both 2ET and DGME, indicating that new *X–Y* interactions were formed [25]. The following data suggests that the interaction between the corresponding polymers AW/PEG is most likely to occur via the C–O group. Liquid surface tension γ together with a shift peak in buffer liquids – hexane and decalin – was used to build a baseline for calculating the magnitude of the corrected peak shift Δv_{xy}. An example of a calculation of the peak shift correction is shown in Fig. 2. The difference of the peak shift in hexane and decalin can be caused by a difference in their chemical structure.

For the calorimetric analysis of a neat liquid *X*, the self-interaction energies were evaluated using the following equations. The total self- interaction energy E_{XX} (J mol^{-1}) is expressed as

$$E_{XX} = \frac{1}{2} N_{Avo} \varepsilon_{XX} \qquad (1)$$

where N_{Avo} is Avogadro's number (6.022 X 10^{23} (particles/mol)) and ε_{XX} is the contact energy of two molecules (or one pair) (J). E_{XX} can be experimentally obtained, when liquid *X* is diluted into a non-self-interacting liquid *Z*, such as hexane. This mixing can be described as

$$N_X(X\text{–}X) + N_Z(Z) \xrightarrow{\ddot{A}H_M} N'_X(X\text{–}X) + N''_X(X) + N_Z(Z) \qquad (2)$$

Table 3
Surface tension γ, peak position v and corrected peak shift Δv_{xy} of low molecular liquid substitutes and solvents

Name	Surface tension γ [mN/m]	Peak position v [cm^{-1}]	Corrected peak shift Δv_{xy} [cm^{-1}]
C–O, 1% 2-ethoxyethanol			
Hexane	18.40	1122	–
Decalin	29.40	1124	–
Methylacetamide	28.20	1115	9.1
C–O, 1% Diethylene glycol monoethyl ether			
Hexane	18.40	1122	–
Decalin	29.40	1124	–
Methylacetamide	31.70	1119	5.2
N–H, 1% methylacetamide			
Hexane	18.40	3295	–
Decalin	29.40	3293	–
Amyl butyrate	25.55	3306	12.1
Butyl valerate	26.36	3308	14.2

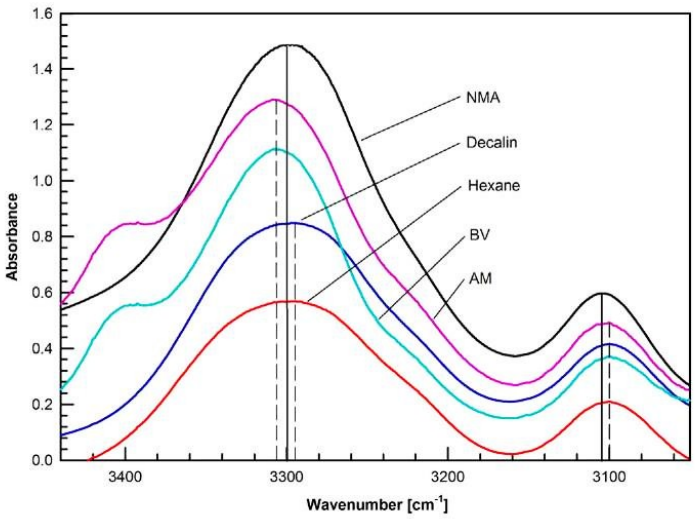

Fig. 1. Shift of FTIR peaks for N–H stretch bonding of 1% methylacetamide (NMA) in hexane, decalin, butyl valerate (BV) and amyl butyrate (AM).

where *(X–X)* means liquid *X* self-associated in *X-X* pairs, while *(X)* means liquid *X* in which molecules are isolated (or dissociated). N_X and N_X' are numbers of *X* molecules (that are associated in *X–X* pairs) before and after mixing, respectively, N_X' stands for the number of X molecules which are isolated after mixing ($N_X = N_X' + N''_X$), ΔH_M represents the heat of mixing. The number of *X-X* pairs before and after mixing NP_{XX} and NP_{XX}', respectively, can be easily obtained ($NP_{XX} = 1/2N_X$; $NP_{XX}' = 1/2N_X'$). Dividing Eq. (2) by N_{AVO} we get

$$n_X(X\text{–}X) + n_Z(Z) \xrightarrow{\ddot{A}H_M} n'_X(X\text{–}X) + n''_X(X) + n_Z(Z) \qquad (3)$$

where n_x means the number of moles of liquid *X*, under the condition that $n_x \ll n_Z$, $n_x' \rightarrow 0$ and $n''_X = n_x$. For $n_x = 1$, ΔH_M becomes E_{xx}. Eq. (3) becomes simpler

$$1(X\text{–}X) + n_Z(Z) \xrightarrow{E_{XX}} 1\,(X) + n_Z(Z) \qquad (4)$$

Experimental data for the dilution of liquid into hexane can be seen in Fig. 3. Trying to describe the shape of the curve, it is convenient to set the axes:

$$x = \frac{n_X}{n_X + n_Z} \qquad y = \frac{\Delta H_M}{n_X + n_Z} \qquad (5)$$

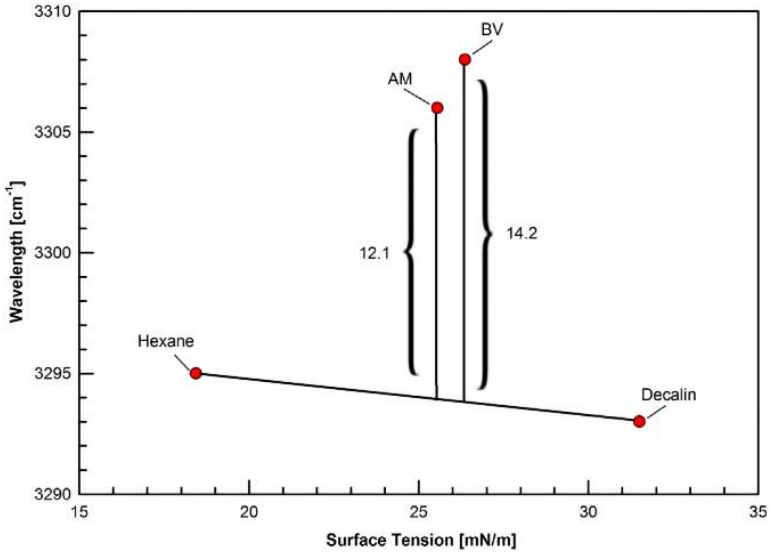

Fig. 2. Calculation of corrected peak shift from the baseline for N-H stretch bonding of 1% methylacetamide (NMA) in hexane, decalin, butyl valerate (BV) and amyl butyrate (AM).

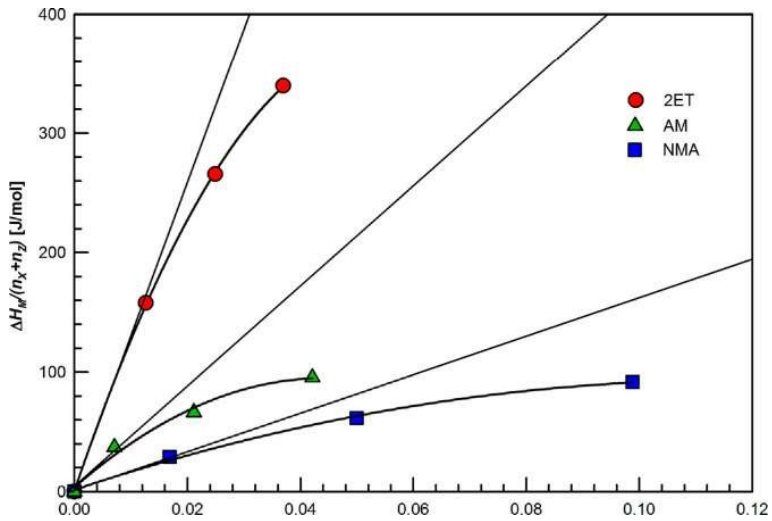

Fig. 3. Heat of mixing $H_M/(n_X + n_Z)$ vs. molar fraction of liquid *X* diluted into solvent *Z* $n_X/(n_x + nz)$.

The shape of the curve can be described as a polynomial by $(y = k_1x + k_2x^2 + ...)$. For $x \rightarrow 0$, higher terms are much smaller than the first term $(k_2x^2 \ll k_1x)$, and the equation becomes linear $(y = k_1x)$. The meaning of the initial slope can be expressed as

$$k_1 = \frac{\Delta y}{\Delta x} = \frac{\frac{\Delta H_M}{n_X + n_Z}}{\frac{n_X}{n_X + n_Z}} = \frac{\Delta H_M}{n_X} \qquad (6)$$

Then the slope is equal to that E_{XX} that is the self-interacting energy of 1 mol of liquid X (J mol^{-1}). The contact energy of two molecules (one pair) of ε_{XX} can be obtained from Eq. (1).

As can be seen from Fig. 3, the association of the heat of mixing and the molar fraction of the dilution are tending to linearity. The less the bending of the curve, the more linear is ΔT. Fig. 4 shows the self- interaction energies of the studied liquids. As can be seen, regardless of their high molecular weight, the self-interaction energies E_{XX} for both AM and BV are significantly smaller than those for 2ET and DGME. This can be explained by the additional –OH in the chemical structure, but it requires a more detailed study. The NMA having the lowest molecular weight among all investigated liquids and shortest chemical chain showed the smallest value of self-interaction energies. It is also possible that particular self-interactions are rather high, and they cannot be broken in the non-polar buffer solution.

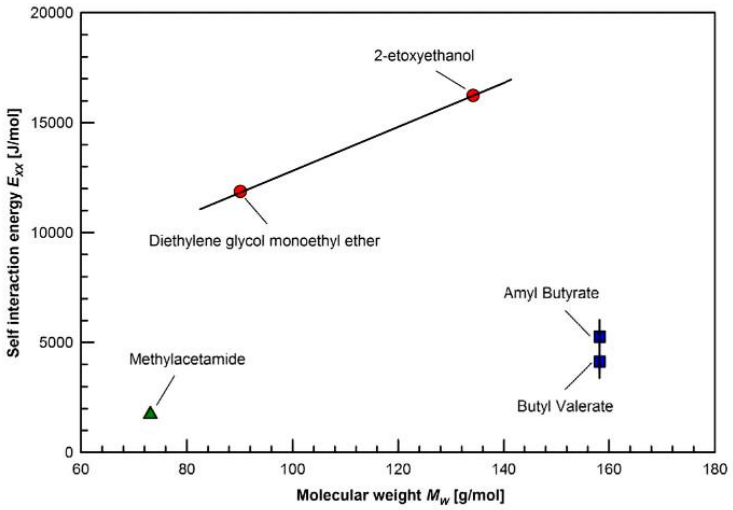

Fig. 4. Self-interaction energies E_{XX} vs. molecular weight M_W for low molecular liquid substitutes.

Similarly, the calorimetric analysis of liquid X mixed with liquid Y can be described as follows (both X and Y have some degree of acid-base self-interactions E_{XX} and E_{YY}). The semichemical equation in this case is

$$N_X(X\text{–}X) + N_Y(Y - Y) \xrightarrow{\ddot{A}H_M} N_{XY}(X\text{–}Y) + N'_X(X - X) + N'_Y(Y - Y) \qquad (7)$$

where N_{XY} is the number of X and Y molecules that are associated in X–Y pairs. The total number of molecules is equal before and after mixing $(N_X + N_y = N_{XY} + N_X' + N_Y')$. The number of X-Y pairs is given by $(NP_{XY} = 1/2N_{XY})$, and the total number of pairs before and after mixing is given by $(NP_{XY} + NP_{YY} = NP_{XY} + NP'_{XX} + NP''_{YY})$. By dividing Eq. (7) by N_{AVO}, we get

$$n_X(X\text{–}X) + n_Y(Y - Y) \xrightarrow{\ddot{A}H_M} n_{XY}(X\text{–}Y) + n'_X(X - X) + n'_Y(Y - Y) \qquad (8)$$

If $n_X \ll n_Y$, then $n_X' \wedge 0$. Setting $n_X = 1$ mol, then

$$1(X-X) + n_Y(Y-Y) \xrightarrow{\ddot{A}H_M} 2(X-Y) + (n_Y - 1)(Y-Y) \quad (9)$$

ΔH_M becomes ΔE_{XY} and the only changing quantities are

$$1(X-X) + 1(Y-Y) \xrightarrow{\ddot{A}E_{XY}} 2(X-Y) \quad (10)$$

A description by self-interaction (E_{XX}) and by association (E_{XY}) energies gives

$$E_{XX} + E_{YY} + \Delta E_{XY} = 2E_{XY} \quad (11)$$

Self-interaction energies (E_{XX}) were obtained by diluting liquid *X* into hexane. The value ΔE_{XY} can be obtained from the slope analysis, similar to the case of diluting of liquid *X* into hexane, but in this case liquid *X* is diluted into liquid *Y*. Continuing the mathematical analysis, the respective interaction energy of 1 mol of *X–Y* pairs can be expressed as

$$E_{XY} = 1/2(E_{XX} + E_{YY} - \Delta E_{XY}) \quad (12)$$

and the respective contact energy of one pair is

$$\varepsilon_{XY} = \frac{2E_{XY}}{N_{AVO}} \quad (13)$$

The comparison of the temperature change for NMA diluted in 2ET and AM is shown in Fig. 5. Each temperature change is generated by placing a 0.05 ml droplet into a 5 ml liquid. A constant increase of temperature during dilution was observed only between NMA-2ET and NMA-DGME. For the dilution of all other compositions, the temperature change was negative. An increase in temperature during mixing can be associated with a strong, newly formed *X–Y* interaction. The background is described in the following two equations.

According to Gibbs free energy, if the change of the ΔG is negative, the reaction can proceed spontaneously. Basically, in the case of mixing it is given by

$$\Delta G_M = \Delta H_M - T\Delta S_M \quad (14)$$

where ΔH_M and ΔS_M are the enthalpy and entropy of mixing, respectively. In binary polymer mixtures, it is convenient to use the Flory and Huggins expression for the Gibbs free energy of mixing per mole of lattice sites

$$\frac{\Delta G_M}{RT(V/V_r)} = \frac{\phi_X}{r_X}\ln\phi_X + \frac{\phi_Y}{r_Y}\ln\phi_Y + X\phi_X\phi_Y \quad (15)$$

where *V* is the total volume, V_r is the molar volume of a segment, and r_X and ϕ_X denote the number of segments per chain and the volume fraction of component *X*, respectively. On the right side of Eq. (15), the first two terms refer to combinatorial entropy, while all noncombinatorial effects are represented by the *x* parameter. The combinatorial entropy of mixing is related to the positional disorder in the system. As the mixture is more disordered than the pure components, the combinatorial entropy of mixing leads to a negative contribution to ΔG_M, i.e., stabilisation of the mixture. However, the combinatorial entropy for the polymer mixture consisting of high molecular weight components (large r_X and r_Y) is virtually zero, and the negative contribution to ΔG_M is comparatively negligibly small due to the mixtures of small molecules [26].

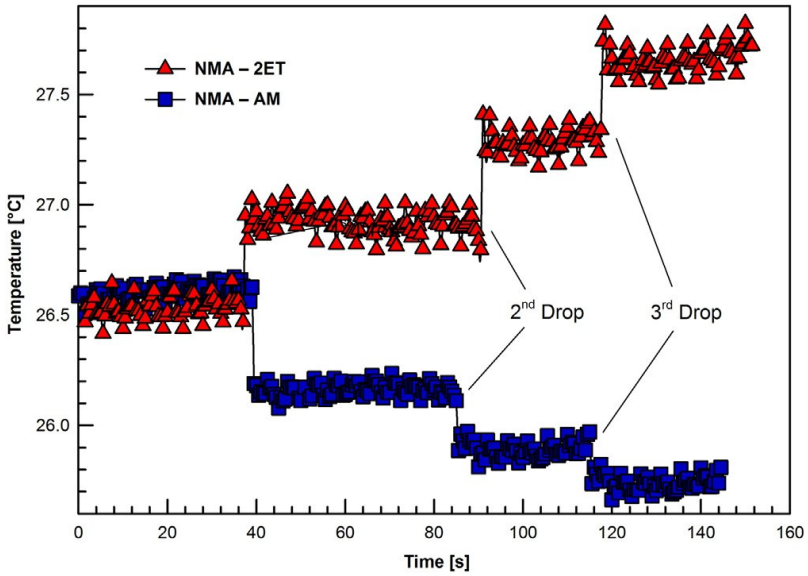

Fig. 5. Temperature change for the 0.05 ml drop of methylacetamide (NMA) diluted in 5 ml 2-ethoxyethanol (2ET) and amyl butyrate (AM).

The temperature drops in a buffer solution and the self-interaction energies (E_{XX}) are shown in Table 4. In order to understand the component fraction of the blend after dilution, the heat of mixing vs. molar fraction and the fraction of liquid X diluted into solvent Z were calculated. A schematic plot (see Fig. 6) shows the principle of calculation of the E_{XY} based on the measurements of ΔE_{XY} according to Eq. (12). An evaluation of E_{XY} for the respective pairs showed that X–Y interaction values are asymmetric. The value for liquid X diluted in liquid Y was slightly different than the value of liquid Y diluted in liquid X. The error was neglected. This could be caused by a difference in the heat capacity c_p of each liquid.

The respective association energies E_{XY} for each X–Y pair evaluated using Eq. (13) are shown in Table 5. The highest values are observed for 2ET-NMA and DGME-NMA blends, 9659 and 7139 [J/mol], respectively, while the smallest interaction energies were observed between DGME and BV with only 3011 [J/mol].

Together, FTIR and calorimetry provide the necessary information for the evaluation of the specific interactions. The shift of peaks in FTIR measurements as well as the observed temperature surge for certain blends with the sole help of analogue calorimetry can serve as proof of the presence of specific interactions, while combing both data together allows the establishment of the relationship of the two independent experiments.

Table 4
Temperature drop ΔT, heat of mixing $\Delta H_M/(n_x+n_z)$, molar fraction $n_x/(n_x+n_z)$ and self-interaction energies E_{XY}.

Name	Temperature change ΔT [°C]	$\Delta H_M/(n_x+n_z)$ [J/mol]	$n_x/(n_x + nz)$ [10^{-3}]	Self-interaction energy E_{xx} [J/mol]
AM	0.19	28.35	6.708	5264
BV	0.15	29.38	6.754	4132
2ET	0.81	157.82	12.633	11,861
DGME	0.80	156.41	9.146	16,236
NMA	0.15	29.14	16.835	2308

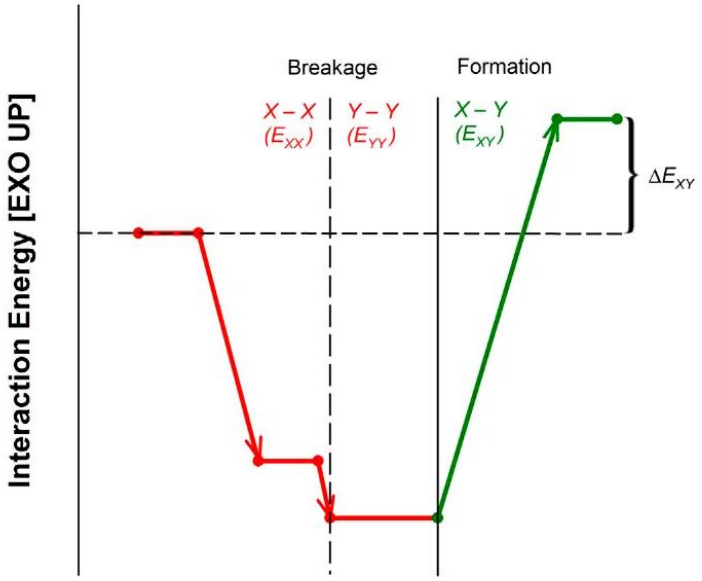

Fig. 6. Simplified schematic of breaking self-interactions *(X–X and Y–Y)* followed by the formation of new *X–Y* interactions during dilution of liquid *X* in liquid *Y* for low molecular substitutes.

The vibrating frequency of a certain group (such as C–O) is given by

$$v = v^{v} + \Delta v^{d} + \Delta v^{\mathrm{ab}} \qquad (16)$$

where v^{v} means the frequency in the vapour phase, Δv^{d} is the frequency shift caused by dispersion force interactions between a certain group and its local environment (non-acid-base interacting liquid such as hexane), and Δv^{ab} means the frequency shift due to acid-base interactions.

When the tested liquid was diluted in non-interacting liquids (such as cyclohexane, heptane, octane, etc.), a linear relationship of Δv^{d} with the dispersion force contribution to the surface tension γ^{d} was found ($\Delta v^{ab} = 0$). In our case, the tested liquids were diluted in two non-interacting liquids (hexane and decalin) with an appreciably different surface tension in order to obtain the linear relationship ($v = v^{v} + a\gamma^{d}$). For the acid-base interacting liquids, the exact values of Δv^{ab} were calculated by the deviation from the linear relationship satisfied in non-interacting liquids [27]. On the basis of quantum mechanics, Drago [28] explained the linear relationship between enthalpy of adduct formation and the shift in the frequency of vibration:

$$\Delta H = k\Delta v^{ab} \qquad (17)$$

The obtained data from two independent experiments can be verified by this relation. The E_{XY} association energies obtained by calorimetry and shifts of peaks Δv^{ab} measured using FTIR are shown in Fig. 7. A linear dependence was found for the tested pairs, confirming the validity of data and calculations from two independent experiments.

Table 5
Association energies E_{XY} of respective pairs *X–Y*

Liquid, [1%]	2ET	DGME	AM	BV	NMA
2ET	–	–	5008	6471	9659
DGME	–	–	3793	3011	7139
AM	5560	4162	–	–	5899
BV	6784	3294	–	–	6353
NMA	10,624	7846	5382	5810	–

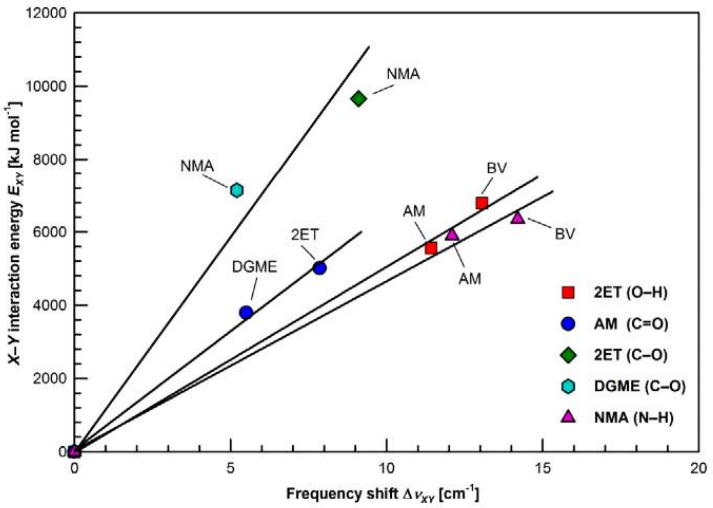

Fig. 7. Association energies E_{XY} vs. shift of peaks for low molecular weight substitutes of acrawax, carnauba wax and polyethylene glycol.

4. Conclusion

Understanding the role of particular binder components is key for the development of novel binder systems with advanced processing properties. Interactions of low molecular weight analogues of polyethyleneglycol (PEG) with acrawax (AW) have been compared with those of carnauba wax (CW) in order to quantify the difference between these two polar waxes. FTIR spectra for substitute liquids of AW and PEG showed a shift of the C-O stretch absorption peak to a lower wave number in a range between 5.2-9.1 cm^{-1}, solely referring to the presence of the interactions between the components. Further, the analogue calorimetric analysis showed a temperature drop for all low molecular compositions (AW/CW, CW/PEG) except for AW/PEG substitutes, which attracted each other more than themselves, expressing an up to 0.52 °C temperature increase during the mixing. The E_{XY} association energies for AW/PEG were on average 2.1 times higher than for CW/PEG substitutes. This can be explained by the presence of a C=O group plus an N-H group for each molecule of the AW analogue in comparison with one C=O group plus one C–O group per molecule of the CW analogue. It is conceivable that a strong type of interactions (such as hydrogen bonding) is formed during AW and PEG mixing. The combination of FTIR and calorimetry data in conjunction with Drago's equation allowed for the defining of the linear relationship of two independent experiments. The final results of the analyses for blends of low-molecular weight analogues suggest that the corresponding AW/PEG polymer blend with higher interactions is more favourable than CW/PEG for powder injection moulding.

Acknowledgments

This article was written with the support of the Operational Program Research and Development for Innovations co-funded by the ERDF and the National Budget of Czech Republic, within the framework of the project Centre of Polymer Systems (reg. number: CZ.1.05/2.1.00/03.0111).

The author D.B. acknowledges the support of an internal grant from TBU in Zlin, IGA/FT/2015/001.

References

[1.] R.M. German, A. Bose, Injection Molding of Metals and Ceramics, Metal Powder Industries Federation, Princeton, N.J., 1997

[2.] S.B. Ren, X.B. He, X.H. Qu, I.S. Humail, Y. Li, Effects of binder compositions on characteristics of feedstocks of microsized sic ceramic injection moulding, Powder Metall. 50 (2007) 255-259.

[3.] J. Hidalgo, C. Abajo, A. Jimenez-Morales, J.M. Torralba, Effect of a binder system on the low-pressure powder injection moulding of water-soluble zircon feedstocks, J. Eur. Ceram. Soc. 33 (2013) 3185-3194.

[4.] R.K. Enneti, T.S. Shivashankar, S.J. Parle, R.M. German, S.V. Atre, Master debinding curves for solvent extraction of binders in powder injection molding, Powder Technol. 228 (2012) 14-17.

[5.] S.M. Ani, A. Muchtar, N. Muhamad, J.A Ghani, Fabrication of zirconia-toughened alumina parts by powder injection molding process: optimized processing parameters, Ceram. Int. 40 (2014) 273-280.

[6.] B. Hausnerova, L. Marcanikova, P. Filip, P. Saha, Optimization of powder injection molding of feedstock based on aluminium oxide and multicomponent water- soluble polymer binder, Polym. Eng. Sci. 119 (2011) 2925-2932.

[7.] J. Hidalgo, A. Jimenez-Morales, J.M. Torralba, Torque rheology of zircon feedstocks for powder injection moulding, J. Eur. Ceram. Soc. 32 (2012) 4063-4072.

[8.] F. Sommer, H. Walcher, F. Kern, M. Maetzig, R. Gadow, Influence of feedstock preparation on ceramic injection molding and microstructural features of zirconia toughened alumina, J. Eur. Ceram. Soc. 34 (2014) 745-751.

[9.] S. Ahn, S.J. Park S. Lee, S.V. Atre, R.M. German, Effect of powders and binders on material properties and molding parameters in iron and stainless steel powder injection molding process, Powder Technol. 193 (2009) 162-169.

[10.] S.M. Ani, A. Muchtar, N. Muhamad, J.A Ghani, Binder removal via a two-stage debinding process for ceramic injection molding parts, Ceram. Int. 40 (2014) 2819-2824.

[11.] C. Quinard, T. Barriere, J.C. Gelin, Development and property identification of 316L stainless steel feedstock for PIM and |jPIM, Powder Technol. 190 (2009) 123-128.

[12.] F. Chen, M.P. Wolcott, Miscibility studies of paraffin/polyethylene blends as form- stable phase change materials, Eur. Polym. J. 52 (2014) 44-52.

[13.] A.H. Doulabi, H. Mirzadeh, M. Imani, Miscibility study of chitosan/polyethylene glycol fumarate blends in dilute solutions, J. Appl. Polym. Sci. 127 (2013) 3514-3521.

[14.] B. Hausnerova, I. Kuritka, D. Bleyan, Polyolefin backbone substitution in binders for low temperature powder injection moulding feedstocks, Molecules 19 (2014) 2748-2760.

[15.] L. Liu, X.L. Ni, H.Q. Yin, X.H. Qu, Moldability of various zirconia micro gears in micro powder injection moulding, J. Eur. Ceram. Soc. 35 (2015) 171-177.

[16.] R.N. French,J.M. Machado, D. Linvien, Miscible polyacetal poly(vinyl phenol) blends. 1. Predictions based on low-molecular-weight analogs, Polymer 33 (1992) 755-759.

[17.] P. Svoboda, J. Kressler, T. Ougizawa, T. Inoue, K. Ozutsumi, FTIR and calorimetric analyses of the specific interactions in poly(epsilon-caprolactone)/poly(styrene- co-acrylonitrile) blends using low molecular weight analogues, Macromolecules 30 (1997) 1973-1979.

[18.] D. Rana, B.M. Mandal, S.N. Bhattacharyya, Analogue calorimetry of polymer blends: poly(styrene-co-acrylonitrile) and poly(phenyl acrylate) or poly(vinyl benzoate), Polymer 37 (1996) 2439-2443.

[19.] L. Bernazzani, C. Cardelli, G. Conti, P. Gianni, Analog calorimetry and uniquac group contributions approaches to the miscibility of PVC with EVA copolymers, J. Therm. Anal. Calorim. 70 (2002) 927-947.
[20.] C. Qin, A.T.N. Pires, L.A Belfiore, Spectroscopic investigations of specific interactions in amorphous polymer-polymer blends — poly(vinylphenol) and poly(vinyl methyl ketone), Macromolecules 24 (1991) 666-670.
[21.] D. Bleyan, P. Svoboda, B. Hausnerova, Specific interactions of low molecular weight analogues of carnauba wax and polyethylene glycol binders of ceramic injection moulding feedstocks, Ceram. Int. 41 (2015) 3975-3982.
[22.] K.C. Hsu, C.C. Lin, G.M. Lo, Effect of wax composition on injection moulding of 304L stainless steel powder, Powder Metall. 37 (1994) 272-276.
[23.] K.L. Mittal, H.R. Anderson, F.M. Fowkes, Acid-Base Interactions: Relevance to Adhesion Science and Technology: In Honor of the 75th Birthday of Professor Frederick M. Fowkes, VSP, Utrecht, 1991.
[24.] Y.N. Sudhakar, M. Selvakumar, Miscibility of chitosan and poly(ethyleneglycol) blends in buffer solution, E-Polymers 12 (2012) 1037-1050.
[25.] W.O. George, P.S. McIntyre, D.J. Mowthorpe, Infrared Spectroscopy, Published on behalf of ACOL by Wiley, Chichester, 1987.
[26.] H.W. Kammer, Thermodynamics of polymer miscibility, Acta Polym. 37 (1986) 1-6.
[27.] F.M. Fowkes, D.O. Tischler, JA Wolfe, L.A Lannigan, C.M. Ademujohn, M.J. Halliwell, Acid-base complexes of polymers, J. Polym. Sci. Polym. Chem 22 (1984) 547-566.
[28.] R.S. Drago, G.C. Vogel, T.E. Needham, 4-Parameter equation for predicting enthalpies of adduct formation, J. Am Chem. Soc. 93 (1971) 6014-6026.